Microsyst Technol
DOI 10.1007/s00542-015-2764-4

TECHNICAL PAPER

Using nanogap in label-free impedance based electrical biosensors to overcome electrical double layer effect

Ali Kemal Okyay[1,2,3] · Oguz Hanoglu[1] · Mustafa Yuksel[4] · Handan Acar[2,3] · Selim Sülek[2,3] · Burak Tekcan[1] · Sedat Agan[5] · Necmi Biyikli[2,3] · Mustafa O. Guler[2,3]

Received: 4 September 2015 / Accepted: 9 December 2015

Abstract Point-of-care biosensor applications require low-cost and low-power solutions. They offer being easily accessible at home site. They are usable without any complex sample handling or any kind of special expertise. Impedance spectroscopy has been utilized for point-of-care biosensor applications; however, electrical double layer formed due to ions in the solution of interest has been a challenge, due to shielding of the electric field used for sensing the target molecules. Here in this study, we demonstrate a nanogap based biosensor structure with a relatively low frequency (1–100 kHz) measurement technique, which not only eliminates the undesired shielding effect of electrical double layer but also helps in minimizing the measurement volume and enabling low concentration (μ molar level) detection of target molecules (streptavidin). Repeatability and sensitivity tests proved stable and reliable operation of the sensors. These biosensors might offer attributes such as low-cost label-free detection, fast measurement and monolithic chip integrability.

✉ Ali Kemal Okyay
aokyay@ee.bilkent.edu.tr

[1] Department of Electrical and Electronics Engineering, Bilkent University, Bilkent, Ankara 06800, Turkey

[2] Institute of Materials Science and Nanotechnology, Bilkent University, Bilkent, Ankara 06800, Turkey

[3] National Nanotechnology Research Center (UNAM), Bilkent University, Bilkent, Ankara 06800, Turkey

[4] Department of Audiology, School of Health, Turgut Özal University, Ankara 06800, Turkey

[5] Department of Physics, Kirikkale University, Kirikkale 71450, Turkey

1 Introduction

Diseases like cancer are a major leading cause of death in today's world. Early detection is extremely important for effective and successful treatments of such diseases (Emery et al. 2014). Point-of-care biosensors can be used in early detection by providing low-cost, low-power and small platforms, which are easily accessible at home site and usable without any complex sample handling or any kind of special expertise (Soper et al. 2006; Wang 2006). Biosensor technologies offer various transduction mechanisms including optical (Geng et al. 2014; Maharana et al. 2014; Ligler and Taitt 2008; Narsaiah et al. 2011) magnetic (Devkota et al. 2014; Li and Kosel 2014; Xie et al. 2011; Yoo et al. 2011) and electrical (Dong et al. 2010; Pui et al. 2013; Guo 2013; Buitrago et al. 2014; Chen et al. 2012) detection. Among these mechanisms, electrical based detection stands out as a strong candidate for point-of-care health applications since it offers simplicity, chip-integrability; and, moreover it is quite inclined to low-cost and low-power platforms.

Biosensors are divided mainly into two categories according to their transduction mechanisms: labeled and label-free detection. Labeled biosensors are less suitable for point-of-care health monitoring applications due to sample handling, time and cost issues; whereas label-free biosensors, allowing simple, fast, and low-cost detection, are more preferable (Daniels and Pourmand 2007).

Impedance spectroscopy is an electrical based technique for characterizing systems of interest. It offers advantages like label-free, low cost, low power requirement, miniaturizable, and chip-integrable detection platforms, which are extremely appealing for point-of-care and early disease detection applications. However, impedance spectroscopy

Published online: 26 December 2015

in ionic solutions is hampered by a charge layer called electric double layer. When two metal plates are immersed in a solution and a voltage is applied between them, ions in the solution start to accumulate near the plates, forming a diffusion layer. In addition, there is a layer of immobile ions on the plates forming the Stern layer. These two layers together are called as electrical double layer. Gouy-Chapman model (Parsons 1990) can be used to understand the effect of this layer on electric field distribution between the plates. The model assumes that the ions behave as point charges and employs the Poisson-Boltzmann equation to predict electric field distribution in the solution. This model provides relatively good predictions for solutions with ionic strengths <0.2 Molar and for applied electrical voltages below 50–80 mV (Butt et al. 2006). This model can be used in this work since the ionic strength is in the order of 10^{-7} M and applied rms voltage is 10 mV. According to this model, the electric field with respect to distance x from an electrode can be expressed as

$$|E| = E_0 e^{\left(-\frac{x}{\lambda_D}\right)} \tag{1}$$

Electric field decays exponentially with increasing distances from the electrode (Eq. 1) and most of the field decays in a region determined by the size of the electrical double layer (Fig. 1). The decaying constant λ_D is called Debye length.

Electrical double layer acts as a shield against the applied electric field. This causes a major problem for the biosensor applications since the electric field applied by the electrodes does not appear on the significant portion of the target medium. There are two ways of dealing with this problem, which are increasing the Debye length and decreasing the electrode separation distance.

Increasing Debye length is possible by decreasing the ionic strength of the solution. For water at 25 °C, Debye length is (Butt et al. 2006),

$$\lambda_D = \frac{0.34\text{nm}}{\sqrt{C\text{L/mol}}} \tag{2}$$

where C is the ionic strength. Debye length for human blood plasma is about 0.78 nm due to the high ionic (like Na^+, K^+, Cl^-) content in it. This is a very short distance and thus, it is hardly possible to apply impedance spectroscopy in human blood as the sample medium. On the other hand, deionized (DI) water is a much better choice for obtaining larger Debye lengths. DI water is simply water purified from its mineral ions such as sodium, calcium, iron, copper, chloride and bromide. Thanks to this purification process, ionic strength can be decreased down to 2×10^{-7} and thereby, Debye lengths as long as 760 nm (only 0.78 nm in human blood plasma) can be obtained. Using DI water (if the measuring scheme allows) can help decreasing the effect of the undesired electrical double layer, however, the separation distance of the electrodes should also be in the order of Debye length to warrant electric field uniformity within the target medium.

Nanogap refers to the gap formed between the two electrodes with the separation distance in the order of nanometers. Nanogap concept, in addition to using DI water as the sample medium, enables all molecules filling the gap experience almost identical electrical conditions, thus producing more uniform sensitivity results. In addition to this, since even a single molecule can occupy a reasonable percent of the little volume inside the nanogap, nanogap biosensors can be extremely sensitive to DNA's, proteins and other biological molecules, which are all in nanoscale. Therefore, the ability of shrinking measurement volumes to nanometer dimensions is also a motivating reason for using nanogap based impedance spectroscopy in detection of low amounts of target molecules.

Benefits of nanogap in impedance spectroscopy can be realized by nanogap devices. Numerous nanogap devices with various fabrication techniques have been reported previously (Chen et al. 2010; Yi et al. 2005; Gu et al. 2009; Nevill et al. 2005). These devices can be categorized as planar or vertical nanogap devices. Planar devices have been fabricated by techniques including lithography or chemical deposition. Although it has been reported that some outstanding results can be obtained with these techniques, they are in general not suitable for high-throughput fabrication. On the other hand, vertical nanogap devices are formed by vertically situated electrodes. They are usually formed by incorporating nanometer height sacrificial layers between the electrodes. Nanogap is formed by removing the sacrificial layer (Schlecht et al. 2007); though, some of it may be preferred to remain as a spacer between the electrodes (Ionescu-Zanetti et al. 2006; Im et al. 2007). Advantage of these devices is that they can use low-cost, mature thin film growth techniques for nanoscale height sacrificial layer. These versatile techniques offer great thickness uniformity and control in addition to cost effectiveness. Thus, vertical nanogap devices have been preferred in nanogap based impedimetric biosensors.

In this work, a nanogap based impedimetric biosensor for streptavidin detection is demonstrated. Biotin-streptavidin system was studied because of their known strong non-covalent interactions in nature (Dissociation constant K_d is on the order of $\approx 10^{-14}$ mol/L). We present design, fabrication, and surface functionalization of the biosensor. The surfaces were characterized by scanning electron microscopy (SEM) and X-ray photoelectron spectroscopy (XPS) analysis. Overall efficiency of the biosensor is analyzed by impedance measurements. Sensitivity tests showed that detection of various streptavidin concentrations from 100 µg/mL to 10 ng/mL is possible. To the best

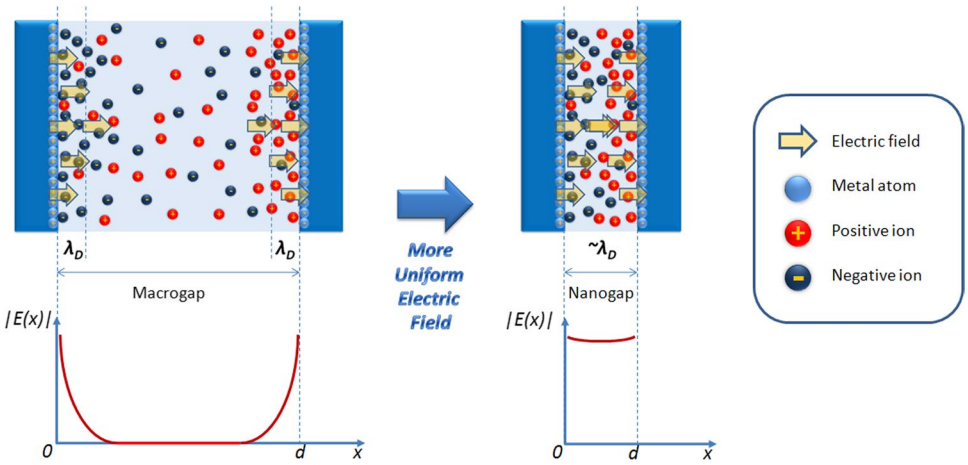

Fig. 1 Electric field intensity between the two electrodes in a solution

of our knowledge, this is the first nanogap based impedimetric sensor showing a ligand–protein binding. Reliability tests proved stable and repeatable operation of the sensors, which are essential for any biosensor platform.

2 Materials and methods

2.1 Design considerations

A vertical nanogap device structure is designed to detect impedimetric changes when target molecules are bound to the recognition elements. Recognition elements are placed on the dielectric layer in between. This dielectric layer functions as a separator for two electrodes, as well as a holder for receptor molecules (Fig. 2).

The measurement volume and the surface area of the recognition elements can be manipulated by the sensor geometry. The electrode geometry shown in Fig. 2d serves the purpose of increasing the percentage of the (target molecule sensing) nanogap area with respect to (insensitive) dielectric material volume, which contributes constant impedance to the overall impedance. The structure in Fig. 2c increases the ratio of sensor perimeter (proportional to nanogap volume) versus sensor area (proportional to dielectric volume) by about 145 times when compared to a square pad occupying the same area. In this design, fingers with high permittivity to area ratio comprise 89 % of the whole area.

2.2 Fabrication of nanogap devices

Nanogap devices were fabricated by consecutive deposition of metal and dielectric layer stack of Cr(10 nm)/Au(100 nm)/Cr(10 nm)/SiO_2(200 nm)/Al_2O_3(40 nm)/Cr(10 nm)/Au(120 nm) followed by a partial sacrificial etching step. Thin Cr layers are used to promote adhesion between Au and oxide layers. Cr and Au layers are deposited by thermal evaporation. $SiO_2$and Al_2O_3 layers were deposited by plasma-enhanced chemical vapor deposition (PECVD) and atomic layer deposition (ALD), respectively. Main aim of the thin alumina layer is to effectively passivate the oxide surface by conformably coating the possible pin-holes formed during PECVD coating process. The top 120-nm-thick Au layer is patterned using standard lift-off process. Using this Au layer as an etch mask, $SiO_2 + Al_2O_3$ layers are partially etched in diluted HF (hydrofluoric acid) solution such that nanogaps were formed at the edges of the electrodes. Formation of the nanogaps is verified by SEM images (Fig. 3).

2.3 Immobilization of biotin on the nanogap surface

For active biosensing model, the oxide layer was functionalized by a surface modification procedure. Theaminopropyltrimethoxysilane (APTS) functionalization procedure was used since it is a well-known, highly efficient surface preparation procedure (Ahluwalia et al. 1992; Ulman 1996). Prior to surface functionalization, the sample was cleaned thoroughly with acetone, 50 % methanol/toluene mix and 100 % toluene respectively (all purchased from Merck). APTS was purchased from Sigma-Aldrich and 5 % APTS (0.213 mM) solution was prepared in toluene. The cleaned sample was immersed into this solution at room temperature for about 5 h. This was followed by exhaustive toluene and methanol rinse and nitrogen blow-drying.

Following the surface functionalization, biotinylation process was started to fix biotin molecules to functionalize walls of the nanogap. The reaction between free carboxylate group of the biotin and free amine group of the APTS on the surface was performed by standard amide formation reaction (Ulman 1996; Acar et al. 2011). Biotinylation solution was prepared by dissolving two equivalents of biotin (purchased from Sigma-Aldrich), 1.95

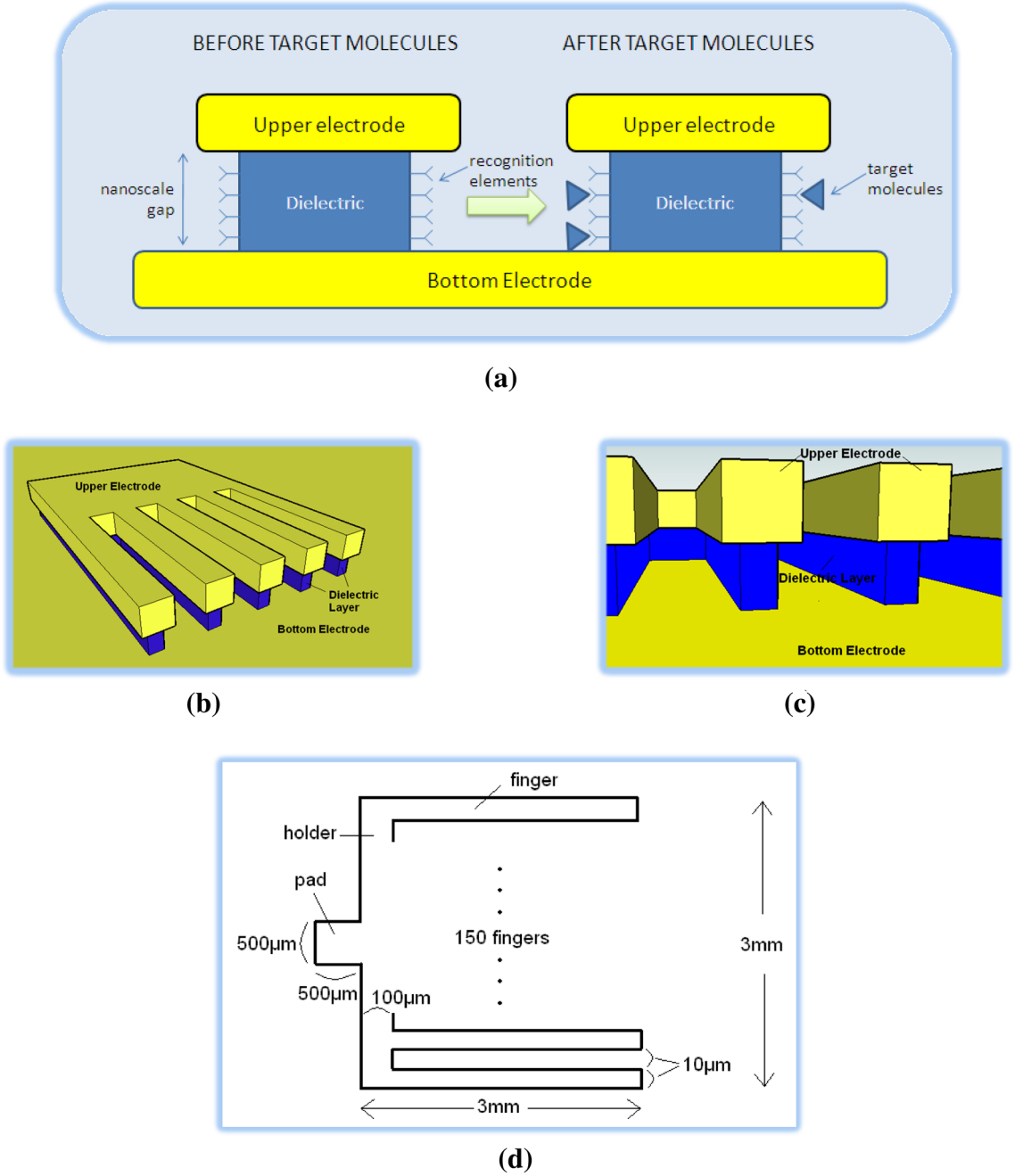

Fig. 2 Operation principles and various views of the designed sensors

equivalents of O-Benzotriazole-N,N,N′,N′-tetramethyl-uronium-hexafluoro-phosphate (HBTU, purchased from ABCR), three equivalents of N,N-diisopropylethylamine (DIEA, purchased from Merck) in 30 mL dimethylformamide (DMF, purchased from Sigma-Aldrich). This amount was sufficient to coat more than ten times the whole APTS on the substrate surface. HBTU and DIEA were used forthe activation of the carboxylate group of biotin for immobilization on the surface. After washing with DMF, the samples were immersed into biotin solution at room temperature for about 2 h. Then, the samples were rinsed with dichloromethane (DCM, purchased from Merck), ethanol, DDW (double distilled water) and blow-dried with nitrogen. Efficiency of the procedure was verified by XPSanalysis. Presence of S atoms was used as an indicator of biotin molecules. Results verified that biotin molecules are present only on the samples with SiO_2 surface as expected.

The above protocol was performed only for once per sample and after the completion of these steps, sensor fabrication is completed and sensors are ready for measurement.

2.4 Measurements: introduction of streptavidin

Measurement procedure starts with the introduction of streptavidin. Streptavidin was purchased from Sigma-Aldrich and used in phospate-buffered saline solution (PBS, pH 7.4). PBS solution was prepared by dissolving 2 g of KCl, 80 g NaCl, 2.4 g of KH_2PO_4 and 14.4 g of K_2HPO_4 in 1000 mL of double distilled water (DDW) (all purchased from Merck). Streptavidin was prepared in different concentrations ranging from 100 µg/mL to 10 ng/mL.

Streptavidin solution was introduced on the surface of the sample by a micropipette and incubated for 10 h. This duration is quite sufficient for streptavidin immobilization to the walls in the nanogap and it can be shortened as well. During the incubation, the sample was preserved in a vacuum-sealed container to avoid evaporation. This was followed by rinsing the sample thoroughly using DI water and blow drying with nitrogen. This step is also helpful for improved selectivity since molecules attached to the surface of the nanogap through nonspecificbinding would be removed after this step.

2.5 Measurements: electrical characterization

A parameter analyzer capable of low-frequency impedance measurements (Keithley 4200-SCS with 4200-CVU) and a manual DC-probe station (Cascade PM-5) are used. Capacitance measurements are performed within the frequency range of 1–100 kHz. The frequency sweep is performed at 19 frequencies (1, 2,…, 10, 20, … 100). Applied ac voltage signal amplitude is 10 mV_{rms}.

The sample is mounted on the vacuum chuck of probe station, and by the help of micromanipulators, micro-needle tips are precisely positioned and connected to the upper and bottom electrode pads for electrical connection to the parameter analyzer. Open circuit and short circuit calibration is performed prior to the measurements. All measurements were conducted in DI water after DIwater rinse and nitrogen dry for repeatability.

3 Results and discussion

Electrical measurements were performed before and after the introduction of streptavidin and compared with each other to detect presence of streptavidin in the nanogap. In order to get capacitance values out of the measured impedance values, designed biosensor structure was modeled with an equivalent circuit model (Fig. 4). Since two electrodes are separated by a distance on the order of Debye length (about 760 nm for DI water), the complex effect of electrical double layer is eliminated in this design. Thus, the overall nanogap is modeled with only its capacitance and resistance connected in parallel.

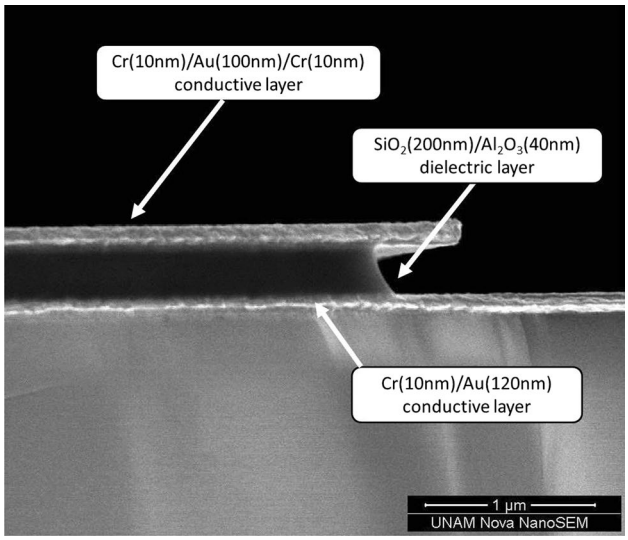

Fig. 3 A cross sectional scanning electron microscope image of the fabricated nanogap biosensors (before surface functionalization)

C_p values were extracted from impedance values by using the model in Fig. 4b. C_p changes with respect to frequency of the applied signal were observed for the five different streptavidin concentrations. The measured capacitance versus frequency curves before and after the application of streptavidin are shown in Fig. 5 for different concentrations of streptavidin solutions. Measured capacitances for all frequencies decrease after streptavidin addition since the streptavidin proteins have lower dielectric constant than the water molecules they displaced ($\varepsilon_{DI\text{-}water} \cong 80$, $\varepsilon_{streptavidin} \cong 2$). It is observed that for the highest streptavidin concentration (100 µg/mL) maximal capacitance change is approximately 1.93 nF, whereas this is 475 pF for the lowest streptavidin concentration (10 ng/mL). Therefore, the biosensor can detect the presence of streptavidin within this range. Upper and lower limits of detection are out of the concentration range considered in this work and dynamic range covers the whole concentration range of 100 µg/mL to 10 ng/mL. However extraction of sensitivity to streptavidin concentration is hindered due to difference in "pre-streptavidin" states (*"pre-streptavidin" plots are not the same for all cases*). This is because the measurements were performed on different sensors of the same wafer and PECVD-coated SiO_2 dielectric film is non-uniform. Figure 5f shows the percentage change in the measured capacitance before and after the application of

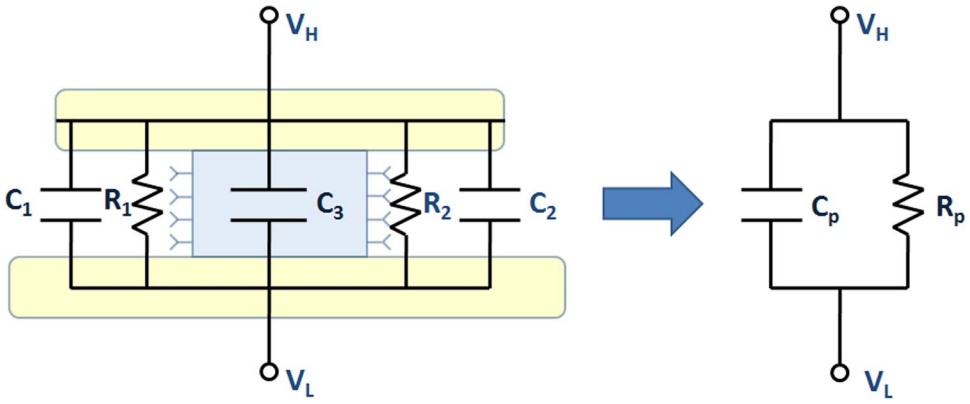

Fig. 4 Equivalent circuit model for the nanogap biosensors in this work **a** Nanogap is modeled with a capacitor (C_1 or C_2) and resistor (R_1 or R_2) in parallel, whereas dielectric layer is modeled with a capacitor (C_3). **b** A more compact equivalent circuit obtained by combining the capacitors and resistors

streptavidin solution. At 10 kHz measurements, the minimum change in the measured capacitance is above 10 % for concentration range of 100 µg/mL to 10 ng/mL. The change in C with concentration of streptavidin proteins at 10 kHz are better separated with respect to 50 kHz measurement. However, for streptavidin concentration quantification purposes, a more linear change is desired. This requires further analysis on almost identical sensors. Looking at the current results, it is not possible to have a conclusion on sensitivity with respect to streptavidin concentration.

Measurement results are consistent with the theoretical estimations. Using the parallel plate capacitor model with undercut length taken as 500 nm (Fig. 3), C_p is estimated to be 2.22 nF. This is very close to the observed capacitance values in Fig. 5, especially at high frequencies. Although nanogap design and DI water measurement medium are preferred to avoid electrical double layer; it seems that this effect is not completely eliminated. However, at higher frequencies, the effect of electrical double layer is less significant due to ionic relaxation (ions cannot respond quickly enough to form electrical double layer) and thus parallel plate model, which assumes no electrical double layer, seems to fit better to the measured results. Nevertheless, high frequencies are not preferable since capacitance change is very small.

The most significant capacitance variations were observed at around 10 kHz. While earlier reports on impedimetric biosensors are generally limited to very high frequencies (>100 MHz) of operation with relatively expensive instruments to eliminate the parasitic contribution of the ions (electrical double layer) in the solution, our current design utilizing the nanogap configuration can be operated at orders of magnitude lower frequencies. Required measurement equipments are relatively low cost when compared to their RF counterparts such as a network analyzer. Moreover, at GHz frequencies, even the metal lines carrying the signal may become problematic due to inductive losses. Thus, special care is required for RF signal handling as well as impedance matching issues to avoid signal reflections. Not only low frequency sensors are easier to handle, but also they are more amenable to chip-integration, which is especially important for point-of-care biosensor applications.

Applied AC voltage signal amplitude is 10 mV_{rms}. This is an advantage of impedance spectroscopy over current–voltage spectroscopy where DC voltage sweep up to several volts are used. As far as biosensing applications are concerned, high voltages would damage the biological structures like proteins. Moreover, system may respond nonlinearly at resulting high electric fields and harmonics of the excitation frequency might be produced.

Reliability tests were performed for the verification of stability and repeatability. Stability tests were performed after biotinylation of sensors. The sample is mounted on the vacuum chuck and probed by micromanipulators. Shortly after starting C_p versus time measurement, DI water is introduced on the sample by a micropipette (Fig. 6a). Signal response is observed for about 20 min, which is a quite long duration considering point-of-care applications where single impedance measurement is enough and can be completed within a second after stabilization is satisfied. However, it is meaningful to test stability for long durations considering clinical applications, where constantly monitoring the concentration of target molecules with respect to time is required. Signal stabilization is satisfied shortly after the application of DI water around 1.67 nF within a tolerance band of ±0.03nF. Signal is sustained within this tolerance range during 20 min time intervals considered. Small changes in the capacitance might be due to non-static ionic distribution created by the rapidly changing electric field.

The response time was measured by analyzing the change in signal response during DI water application and observed to be <10 s (Fig. 6b). This is mainly the time for DI water filling the nanogap. Repeatability was tested by changing the measurement medium from air to

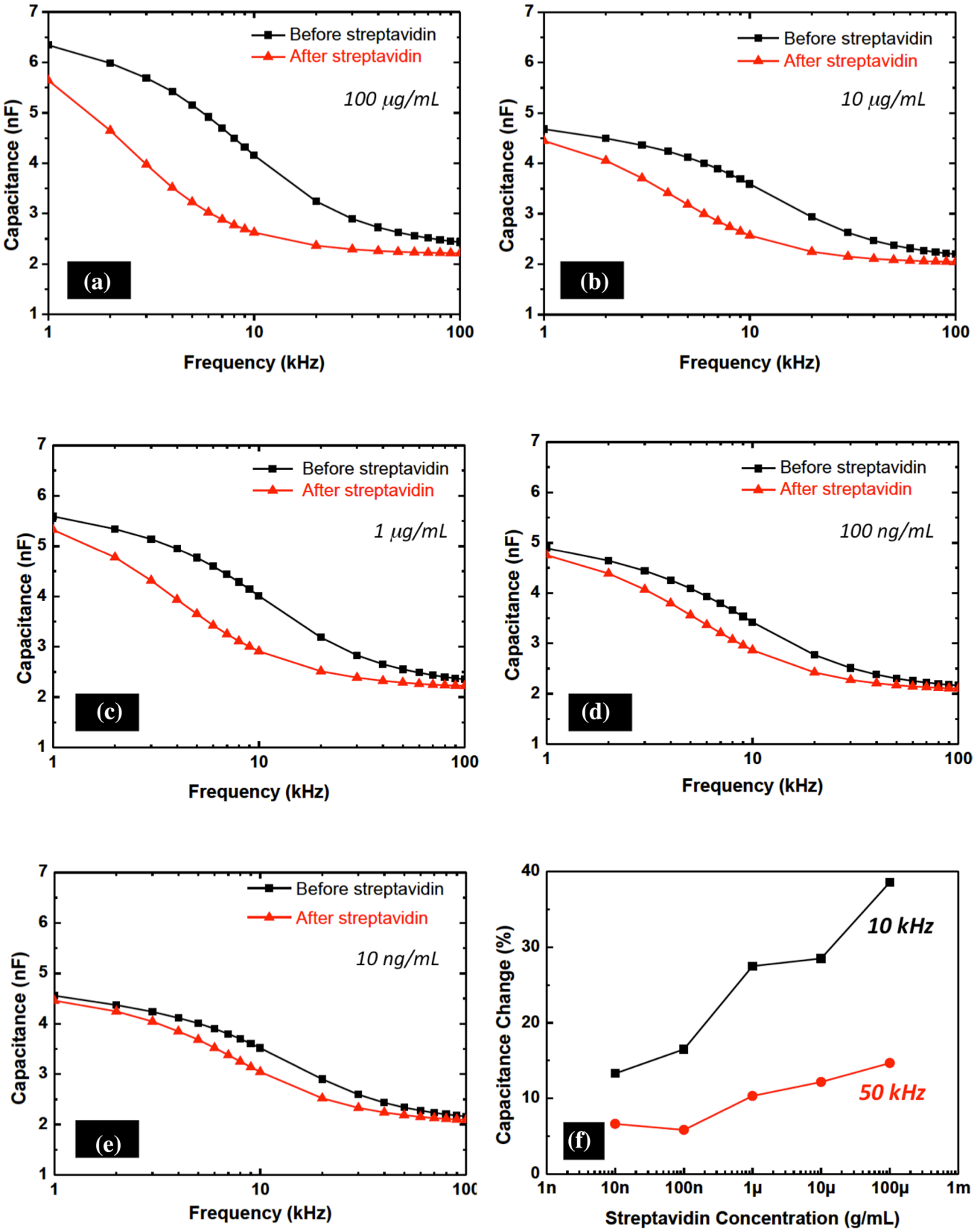

Fig. 5 **a**–**e** Capacitance (C_p) versus frequency (f) for different concentrations of streptavidin solution. For all concentrations, significant changes in the capacitances are observed after streptavidin proteins are bound to the biotin molecules. **f** Percentage change in the measured capacitance before and after the application of streptavidin solution at 10 and 50 kHz

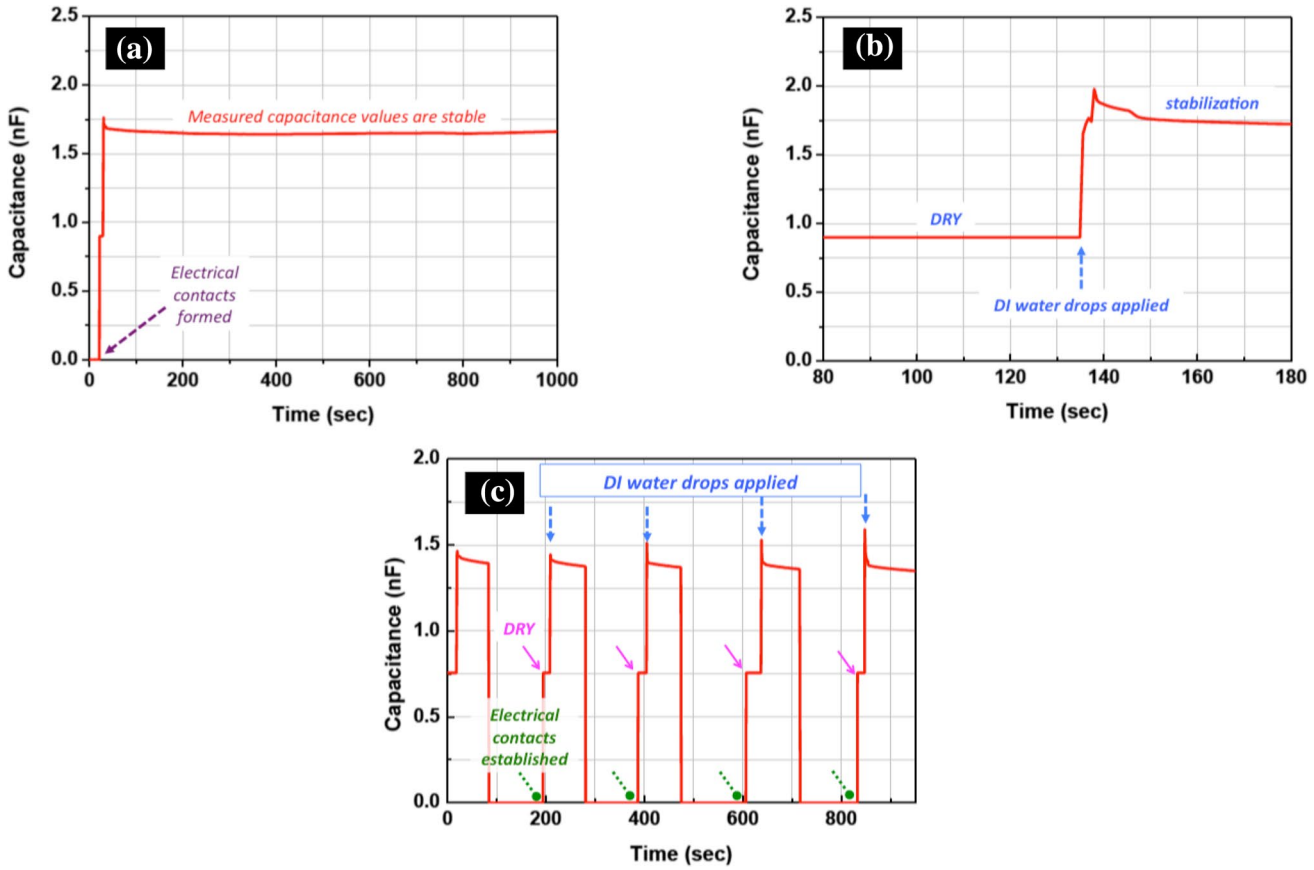

Fig. 6 Reliability tests (**a**) C_p versus time is analyzed for more than 20 min for stability verification. DI water is used as the medium and excitation frequency is 50 kHz. **b** A closer view of the duration before and after the application of DI water. **c** Repeated dry-wet cycle to investigate repeatability performance of the sensors

DI water (by wetting with a micropipette) and DI water to air (by drying with a nitrogen gun) (Fig. 6c). These tests were also performed on other sensors on the same wafer and similarly, stable and reproducible results were observed.

4 Conclusions

Here, we demonstrated nanogap based impedimetric sensor for streptavidin detection. Sensitivity tests revealed detection of various streptavidin concentrations from 100 µg/mL to as low as 10 ng/mL is possible. Reliability tests proved stable and repeatable operation of the sensors. Electrical double layer formed due to ions in the solution of interest is problematic since it shields the applied electric field. Nanogap allows eliminating this problem at low frequencies, which gives the opportunity of chip-integrality for point-of-care biosensors. Nanogap based biosensor structure has enabled minimizing the measurement volume and promising for low concentration target molecule detection. Measurement method is designed such that after the application of target solution, DI water medium is used for obtaining electrical double layer free measurements. This is also beneficial in increasing the dielectric constant contrasts between the target molecules and medium of measurement and thereby, improving sensitivity. Moreover, this measurement protocol includes DI water rinse step, which serves the purpose of selectivity by removing the unspecifically bound molecules from the measurement medium. These biosensors are also appealing because they are operating at 10 mV_{rms} and offer low-power platforms. The current platform can be integrated with a microfluidic system and a low-cost commercial capacitance chip. This combination can offer novel and beneficial systems for the purpose of point-of-care and early disease detection.

Acknowledgments This work was supported in part by European Union Framework Program 7 Marie Curie IRG Grant 239444 and 249196, COST NanoTP, TUBITAK Grants 109E044, 112M004, 112E052, 112M944 and 113M815. The authors acknowledge support from TUBITAK-BIDEB. The authors thank FiratYilmaz for his contributions and Dr. Mohammad Ghaffari for SEM images.

References

Acar H, Garifullin R, Guler MO (2011) Self-assembled template-directed synthesis of one-dimensional silica and titania nanostructures. Langmuir 27(3):1079–1084

Ahluwalia A, De Rossi D, Ristori C, Schirone A, Serra G (1992) A comparative study of protein immobilization techniques for optical immunosensors. Biosens Bioelectron 7(3):207–214

Buitrago E, Badia MF-B, Georgiev YM, Yu R, Lotty O, Holmes JD, Nightingale AM, Guerin HM, Ionescu AM (2014) Electrical characterization of high performance, liquid gated vertically stacked SiNW-based 3D FET biosensors. Sens Actuators B Chem 199:291–300

Butt H-J, Graf K, Kappl M (2006) Physics and chemistry of interfaces, 2nd edn. Wiley-VCH, Weinheim

Chen X, Guo Z, Yang G-M, Li J, Li M-Q, Liu J-H, Huang X-J (2010) Electrical nanogap devices for biosensing. Mater Today 13(11):28–41

Chen Y, Wong CC, Pui TS, Nadipalli R, Weerasekera R, Chandran J, Yu H, Rahman ARA (2012) CMOS high density electrical impedance biosensor array for tumor cell detection. Sens Actuators B Chem 173:903–907

Daniels JS, Pourmand N (2007) Label-free impedance biosensors: opportunities and challenges. Electroanalysis 19(12):1239–1257

Devkota J, Mai TTT, Stojak K, Ha PT, Pham HN, Nguyen XP, Mukherjee P, Srikanth H, Phan MH (2014) Synthesis, inductive heating, and magnetoimpedance-based detection of multifunctional Fe3O4 nanoconjugates. Sens Actuators B Chem 190:715–722

Dong X, Shi Y, Huang W, Chen P, Li L-J (2010) Electrical detection of DNA hybridization with single-base specificity using transistors based on CVD-grown graphene sheets. Adv Mater 22(14):1649–1653

Emery JD, Shaw K, Williams B, Mazza D, Fallon-Ferguson J, Varlow M, Trevena LJ (2014) The role of primary care in early detection and follow-up of cancer. Nat Rev Clin Oncol 11(1):38–48

Geng Z, Kan Q, Yuan J, Chen H (2014) A route to low-cost nanoplasmonic biosensor integrated with optofluidic-portable platform. Sens Actuators B Chem 195:682–691

Gu B, Park TJ, Ahn J-H, Huang X-J, Lee SY, Choi Y-K (2009) Nanogap field-effect transistor biosensors for electrical detection of avian influenza. Small 5(21):2407–2412

Guo X (2013) Single-molecule electrical biosensors based on single-walled carbon nanotubes. Adv Mater 25(25):3397–3408

Im H, Huang X-J, Gu B, Choi Y-K (2007) A dielectric-modulated field-effect transistor for biosensing. Nat Nano 2(7):430–434

Ionescu-Zanetti C, Nevill JT, Carlo DD, Jeong KH, Lee LP (2006) Nanogap capacitors: sensitivity to sample permittivity changes. J Appl Phys 99(2):024305

Li F, Kosel J (2014) An efficient biosensor made of an electromagnetic trap and a magneto-resistive sensor. Biosens Bioelectron 59:145–150

Ligler FS, Taitt CR (2008) Optical biosensors: today and tomorrow. Elsevier, Amsterdam

Maharana PK, Jha R, Palei S (2014) Sensitivity enhancement by air mediated graphene multilayer based surface plasmon resonance biosensor for near infrared. Sens Actuators B Chem 190:494–501

Narsaiah K, Jha SN, Bhardwaj R, Sharma R, Kumar R (2011) Optical biosensors for food quality and safety assurance—a review. J Food Sci Technol 49(4):383–406

Nevill JT, Jeong KH, Lee LP (2005) Ultrasensitive nanogap biosensor to detect changes in structure of water and ice. In: The 13th international conference on solid-state sensors, actuators and microsystems, 2005. Digest of technical papers. TRANSDUCERS'05, 2005 (vol 2), pp 1577–1580

Parsons R (1990) The electrical double layer: recent experimental and theoretical developments. Chem Rev 90(5):813–826

Pui TS, Chen Y, Wong CC, Nadipalli R, Weerasekera R, Arya SK, Yu H, Rahman ARA (2013) High density CMOS electrode array for high-throughput and automated cell counting. Sens Actuators B Chem 181:842–849

Schlecht U, Malavé A, Gronewold TMA, Tewes M, Löhndorf M (2007) Detection of Rev peptides with impedance-sensors—comparison of device-geometries. Biosens Bioelectron 22(9–10):2337–2340

Soper SA, Brown K, Ellington A, Frazier B, Garcia-Manero G, Gau V, Gutman SI, Hayes DF, Korte B, Landers JL, Larson D, Ligler F, Majumdar A, Mascini M, Nolte D, Rosenzweig Z, Wang J, Wilson D (2006) Point-of-care biosensor systems for cancer diagnostics/prognostics. Biosens Bioelectron 21(10):1932–1942

Ulman A (1996) Formation and structure of self-assembled monolayers. Chem Rev 96(4):1533–1554

Wang J (2006) Electrochemical biosensors: towards point-of-care cancer diagnostics. Biosens Bioelectron 21(10):1887–1892

Xie J, Liu G, Eden HS, Ai H, Chen X (2011) Surface-engineered magnetic nanoparticle platforms for cancer imaging and therapy. Acc Chem Res 44(10):883–892

Yi M, Jeong K-H, Lee LP (2005) Theoretical and experimental study towards a nanogap dielectric biosensor. Biosens Bioelectron 20(7):1320–1326

Yoo D, Lee J-H, Shin T-H, Cheon J (2011) Theranostic magnetic nanoparticles. Acc Chem Res 44(10):863–874